Nuclear Reactor Theory Project #1
Group #3

Lee, Seungsup Miller, Dory Payant, Andrew Powers-Luhn, Justin Zhang, Fan

Material	$\Sigma_{tr}(\mathrm{cm}^{-1})$	$\Sigma_a(\mathrm{cm}^{-1})$	$\nu\Sigma_f(\mathrm{cm}^{-1})$	*Relative Absorption*
H	1.79×10^{-2}	8.08×10^{-3}	0	0.053
O	7.16×10^{-3}	4.90×10^{-6}	0	0
Zr	2.91×10^{-3}	7.01×10^{-4}	0	0.005
Fe	9.46×10^{-4}	3.99×10^{-3}	0	0.026
^{235}U	3.08×10^{-4}	9.24×10^{-2}	0.145	0.602
^{238}U	6.95×10^{-3}	1.39×10^{-2}	1.20×10^{-2}	0.091
^{10}B	8.77×10^{-6}	3.41×10^{-2}	0	0.223
	3.62×10^{-2}	0.1532	0.1570	1.000

TABLE I: Macroscopic Cross Sections

I. Introduction & Background

Proving the capabilities and safety of a reactor design requires effective modeling of the neutron flux in the core (expressed in equation 1). For real cores, however, this is impossible, and must be first simplified, then discretized to provide the solution for a representative mesh. Simplifications that can be applied are:

1) **Isotropic assumption**: ignoring the direction of the incoming neutron. This effectively drops all terms involving $\hat{\Omega}$
2) **Monoenergetic assumption**: ignoring the energy variance of the neutrons. This means that a single set of cross sections can be used and allows us to ignore neutrons scattering into and out of the domain of interest
3) **Homogeneity assumption**: assuming that all core materials are evenly mixed throughout the volume of interest. This allows us to ignore discrete boundaries between materials
4) **Steady-state assumption**: assuming that the system has been in this state for a long period and that no transients occur. This allows us to remove all the time dependent terms.

For this project we have analyzed a simplified, monoenergetic, non-multiplying medium in one dimension. The flux originates from a single source at $x = 0$ with a strength of $S = 1 \times 10^8\,\mathrm{s}^{-1}$. These assumptions simplify the transport equation to that presented in equation 2.

In the following sections, we will first describe the terms in equation 2, then provide both an analytical and a discrete solution. We will also provide an analysis of the accuracy of the analysis as a function of the number of nodes. Finally, we will analzye the solution to equation 2 for different coordinate systems.

$$\frac{\partial n}{\partial t} + v\hat{\Omega}\cdot\nabla n + v\Sigma_t n\left(\mathbf{r}, E', \hat{\Omega}, t\right) = \int_{4\pi} d\hat{\Omega}' \int_0^\infty dE' v' \Sigma_s \left(E' \to E, \hat{\Omega}' \to \hat{\Omega}\right) n\left(\mathbf{r}, E', \hat{\Omega}', t\right) + s\left(\mathbf{r}, E, \hat{\Omega}, t\right) \quad (1)$$

$$-D_m \frac{\mathrm{d}^2\phi}{\mathrm{d}x^2} + \Sigma_a^m \phi = \begin{cases} S & (x = 0) \\ 0 & (x > 0) \end{cases} \quad (2)$$

II. Methodology

Equation 2 is a simplified description of neutron diffusion through a finite medium, similar to a point source travelling through a shielding material to a detector. The flux, therefore, depends on the transport cross section. This is accounted for in the term D_m, which is related to the transport coefficient by $D_m = 3\Sigma_{tr}^{-1}$. Values for Σ_{tr} for typical reactor materials are found in table I.

A. Analytic Solution

In the slab, equation 2 is equal to 0, $-D_m \frac{\partial^2\phi}{\partial x^2} + \Sigma_a^m \phi = 0$. In order to better group constants, specify a diffusion length, $L = \sqrt{D_m/\Sigma_a}$. We can then solve for $\phi(x)$:

$$\frac{\partial^2\phi}{\partial x^2} - \frac{\phi}{L} = 0$$
$$\phi(x) = A\mathrm{e}^{-x/L} + C\mathrm{e}^{x/L} \quad (3)$$

First use the boundary condition $\phi(w) = 0$ to solve for C

$$0 = A\mathrm{e}^{-w/L} + C\mathrm{e}^{w/L}$$
$$C = -A\mathrm{e}^{2w/L}$$

Next, use the fact that $-D_m\phi'(0) = J(0) = S/2$ to solve for A

$$J(0) = \frac{S}{2} = -\frac{A}{L}\left(1 + \mathrm{e}^{-2w/L}\right) \tag{4}$$
$$A = \frac{SL}{2D_m}\left(1 + \mathrm{e}^{-2w/L}\right)^{-1}$$

Substituting this in to equation 3, we get:

$$\phi(x) = \frac{SL}{2D_m}\left(\frac{\mathrm{e}^{-x/L} - \mathrm{e}^{(x-2w)/L}}{1 - \mathrm{e}^{-2w/L}}\right) \tag{5}$$

B. Numerical Approximation

It is rare to be faced with a design that allows for an analytical solution. Fortunately, numerical analysis methods exist that allow for approximation of the analytical solution. By dividing our hypothetical medium into discrete sections with nodes at the boundaries between these sections, it is possible to express the flux vector with equation 6:

$$\mathbf{A}\vec{\phi} = \vec{S} \tag{6}$$

where $\vec{\phi}$ is the flux at each node. The operator $\mathbf{A}$ can be derived using the two-node approximation of the second derivative formula:

$$\left.\frac{\partial^2\phi}{\partial x^2}\right|_i \approx \frac{\phi_{i-1} - 2\phi_i + \phi_{i+1}}{\Delta x^2}$$

For non-edge nodes, this can be derived as follows:

$$\begin{aligned}
-D_m\frac{\mathrm{d}^2\phi}{\mathrm{d}x^2} + \Sigma_a\phi &= 0 \\
-D_m\int_{x_i-\frac{\Delta x}{2}}^{x_i+\frac{\Delta x}{2}}\frac{\mathrm{d}^2\phi}{\mathrm{d}x^2}dx + \int_{x_i-\frac{\Delta x}{2}}^{x_i+\frac{\Delta x}{2}}\Sigma_a\phi dx &= 0 \\
-D_m\left.\frac{\mathrm{d}\phi}{\mathrm{d}x}\right|_{x_i-\frac{\Delta x}{2}}^{x_i+\frac{\Delta x}{2}} + \int_{x_i-\frac{\Delta x}{2}}^{x_i+\frac{\Delta x}{2}}\Sigma_a\phi dx &= 0 \\
-D_m\left(\frac{\phi_{i+1}-\phi_i}{\Delta x} - \frac{\phi_i - \phi_{i-1}}{\Delta x}\right) + \int_{x_i-\frac{\Delta x}{2}}^{x_i+\frac{\Delta x}{2}}\Sigma_a\phi dx &= 0 \\
-D_m\left(\frac{\phi_{i+1}-\phi_i}{\Delta x} - \frac{\phi_i - \phi_{i-1}}{\Delta x}\right) + \Sigma_a\phi_i\Delta x &= 0
\end{aligned}$$

Dividing each term by Δx gives:

$$\left(\frac{-D_m}{\Delta x^2}\right)\phi_{i-1} + \left(\frac{2D_m}{\Delta x^2} + \Sigma_a\right)\phi_i + \left(\frac{-D_m}{\Delta x^2}\right)\phi_{i+1} = 0$$

From this we see that our operator $\mathbf{A}$ will have non-corner terms:

$$\begin{bmatrix}
\cdots & \cdots & \cdots & \cdots & \cdots \\
\frac{-D_m}{\Delta x^2} & \frac{2D_m}{\Delta x^2} + \Sigma_a & \frac{-D_m}{\Delta x^2} & 0 & \cdots \\
0 & \frac{-D_m}{\Delta x^2} & \frac{2D_m}{\Delta x^2} + \Sigma_a & \frac{-D_m}{\Delta x^2} & \cdots \\
 & & \ddots & & \\
\cdots & 0 & \frac{-D_m}{\Delta x^2} & \frac{2D_m}{\Delta x^2} + \Sigma_a & \frac{-D_m}{\Delta x^2} \\
\cdots & \cdots & \cdots & \cdots & \cdots
\end{bmatrix}$$

We then solve for our top row using the boundary condition in equation 4:

$$\begin{aligned}
-D_m\frac{\phi_1 - \phi_0}{\Delta x} + D_m\left.\frac{\mathrm{d}\phi}{\mathrm{d}x}\right|_0 + \int_0^{\Delta x/2}\Sigma_a\phi dx &= 0 \\
-D_m\frac{\phi_1 - \phi_0}{\Delta x} + D_m\frac{S}{2} + \int_0^{\Delta x/2}\Sigma_a\phi dx &= 0 \\
-D_m\frac{\phi_1 - \phi_0}{\Delta x} + D_m\frac{S}{2} + \Sigma_a\phi_0\int_0^{\Delta x/2}dx &= 0
\end{aligned}$$

Divide by Δx on both sides:

$$-D_m \frac{\phi_1 - \phi_0}{\Delta x^2} - \frac{S}{2\Delta x} + \frac{1}{2}\Sigma_a \phi_0 = 0$$
$$\frac{-D_m}{\Delta x^2}\phi_1 + \left(\frac{D}{\Delta x^2} + \frac{1}{2}\Sigma_a\right)\phi_0 = 0$$

This gives a final matrix $\mathbf{A}$ (for $n = 5$ nodes):

$$\begin{bmatrix} \frac{D_m}{\Delta x^2} + \frac{1}{2}\Sigma_a & \frac{-D_m}{\Delta x^2} & 0 & 0 \\ \frac{-D_m}{\Delta x^2} & \frac{2D_m}{\Delta x^2} + \Sigma_a & \frac{-D_m}{\Delta x^2} & 0 \\ 0 & \frac{-D_m}{\Delta x^2} & \frac{2D_m}{\Delta x^2} + \Sigma_a & \frac{-D_m}{\Delta x^2} \\ 0 & 0 & \frac{-D_m}{\Delta x^2} & \frac{2D}{\Delta x^2} + \Sigma_a \end{bmatrix}$$

Additional analysis was performed assuming the presence of a source of strength $f \times S$ located at $x = W$. This produced an operator with matrix values (this time for the $n = 4$ case):

$$\begin{bmatrix} \frac{D_m}{\Delta x^2} + \frac{1}{2}\Sigma_a & \frac{-D_m}{\Delta x^2} & 0 & 0 \\ \frac{-D_m}{\Delta x^2} & \frac{2D_m}{\Delta x^2} + \Sigma_a & \frac{-D_m}{\Delta x^2} & 0 \\ 0 & \frac{-D_m}{\Delta x^2} & \frac{2D_m}{\Delta x^2} + \Sigma_a & \frac{-D_m}{\Delta x^2} \\ 0 & 0 & \frac{-D_m}{\Delta x^2} & \frac{D_m}{\Delta x^2} + \frac{1}{2}\Sigma_a \end{bmatrix}$$

In this case the source vector, $\vec{S}$, would follow the form:

$$\begin{bmatrix} \frac{S}{2\Delta x} & 0 & \dots & 0 & f\frac{S}{2\Delta x} \end{bmatrix}$$

Similar derivations (attached) were performed for cylindrical and spherical coordinate systems. The operators for these (in the $n = 4$ case) were, for cylindrical:

$$\begin{bmatrix} \frac{D_m}{\Delta x^2} + \frac{1}{2}\Sigma_a & \frac{-D_m}{\Delta x^2}\left[1 + \frac{1}{2*i+1}\right] & 0 & 0 \\ \frac{-D_m}{\Delta x^2}\left[1 - \frac{1}{2*i-1}\right] & \frac{2D_m}{\Delta x^2} + \Sigma_a & \frac{-D_m}{\Delta x^2}\left[1 + \frac{1}{2*i+1}\right] & 0 \\ 0 & \frac{-D_m}{\Delta x^2}\left[1 - \frac{1}{2*i-1}\right] & \frac{2D_m}{\Delta x^2} + \Sigma_a & \frac{-D_m}{\Delta x^2}\left[1 + \frac{1}{2*i+1}\right] \\ 0 & 0 & \frac{-D_m}{\Delta x^2}\left[1 - \frac{1}{2*i-1}\right] & \frac{D_m}{\Delta x^2} + \frac{1}{2}\Sigma_a \end{bmatrix}$$

and for spherical:

$$\begin{bmatrix} \frac{D_m}{\Delta x^2} + \frac{1}{2}\Sigma_a & \frac{-D_m}{\Delta x^2}\left[1 + \frac{2}{2*i+1}\right] & 0 & 0 \\ \frac{-D_m}{\Delta x^2}\left[1 - \frac{2}{2*i-1}\right] & \frac{2D_m}{\Delta x^2} + \Sigma_a & \frac{-D_m}{\Delta x^2}\left[1 + \frac{2}{2*i+1}\right] & 0 \\ 0 & \frac{-D_m}{\Delta x^2}\left[1 - \frac{2}{2*i-1}\right] & \frac{2D_m}{\Delta x^2} + \Sigma_a & \frac{-D_m}{\Delta x^2}\left[1 + \frac{2}{2*i+1}\right] \\ 0 & 0 & \frac{-D_m}{\Delta x^2}\left[1 - \frac{2}{2*i-1}\right] & \frac{D_m}{\Delta x^2} + \frac{1}{2}\Sigma_a \end{bmatrix}$$

We see here that the spherical and cylindrical coordinate systems introduce additional dependence on $\frac{1}{r}$, as expected from their derivations (included as attachments).

III. Results

A Fortran program was developed to implement the discrete solution to the transport equation from section II-B. The source code is included as an attachment to this report. The numerical solution produced values that converged as the number of nodes increased, showing clearly exponential behavior as $n \to \infty$. This behavior can be seen in figures 1 and 2.

We have also examined this solution analytically in different coordinate systems, specifically cartesian, cylindrical, and spherical. The output of these solutions is easily seen in figure 3. Of note, the derivation for spherical coordinates did not allow for incorporation of the boundary condition $\phi(W) = 0$, which may account for the difference in that curve. A plot was generated showing the predicted flux from the numeric solutions for each of the three coordinate systems. In figure 4 we see that the coordinate systems vary when close to $x = 0$ but converge closer to $x = W$.

From figure 4 it is easy to see parallels with the situations in which one might select these coordinate systems: cartesian for a plane source, cylindrical for a line source, and spherical for a point source.

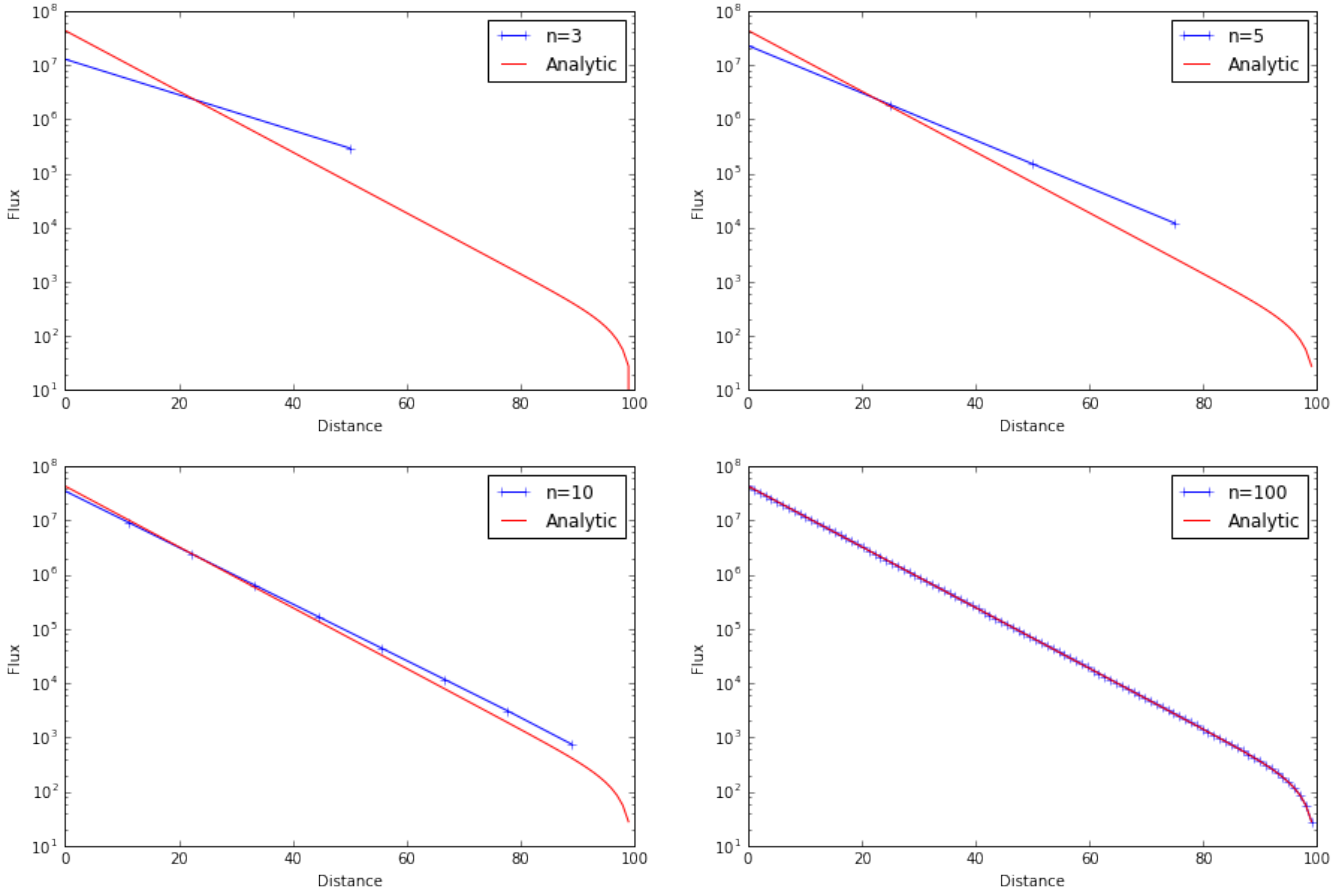

Fig. 1: Comparison of Numerical and Analytical Solutions

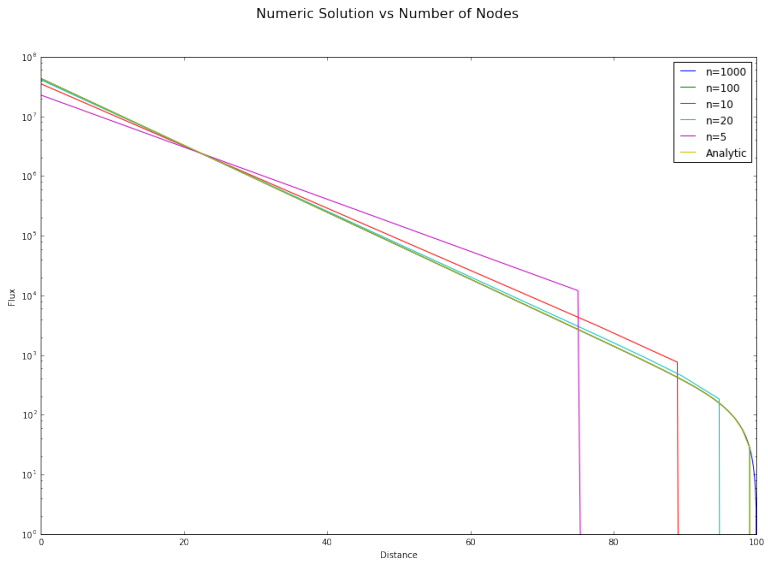

Fig. 2: Change in solution based on number of nodes

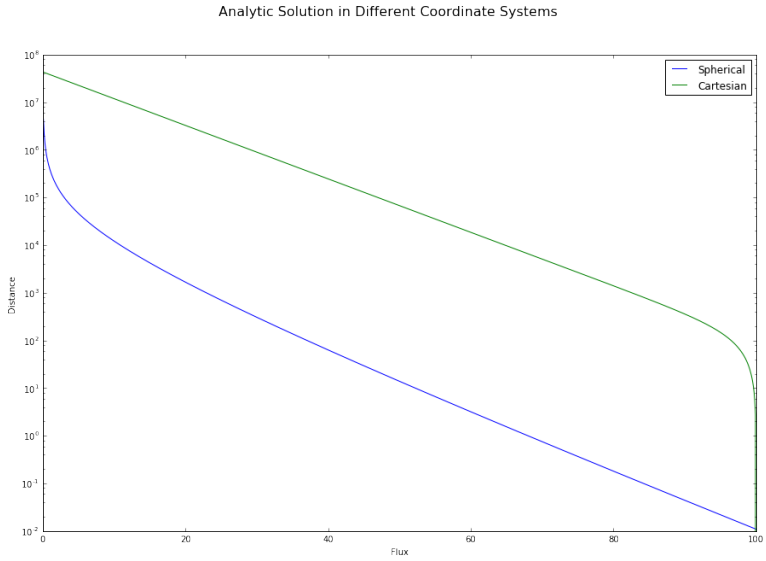

Fig. 3: Analytical Solution for Cartesian and Spherical Coordinates

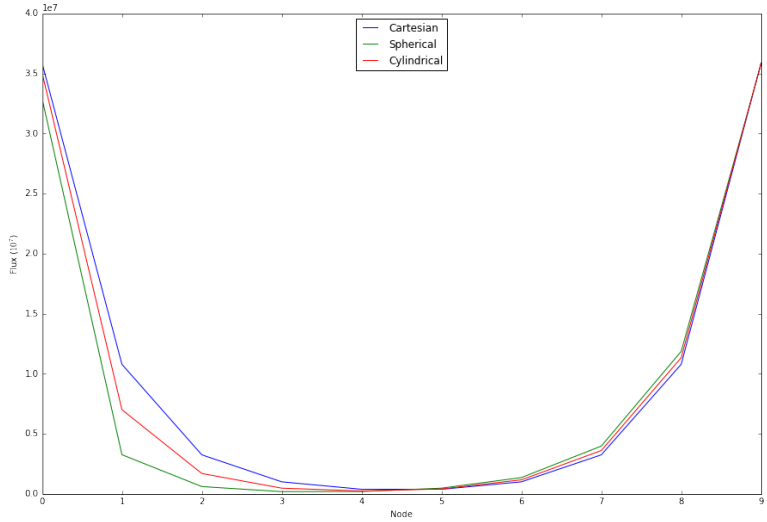

Fig. 4: Numeric Solution for Cartesian, Cylindrical, and Spherical Coordinates

IV. Conclusions

We provide an analysis of a simplified one-group, one-dimensional neutron diffusion in a non-multiplying medium. Solutions are compared in assorted coordinate systems and for numerical approximation of the analytic solution. The various approaches to this problem produced similar but slightly different solutions, implying that careful choice of methodology is necessary in solving similar problems. For simple problems, such as the case with a single source at $x = 0$, the analytical method was less computationally expensive, especially as the number of nodes increased to allow for convergence by the numerical method. It is easy to see the power of the numeric, discrete approach as the system being examined grows in complexity, as demonstrated in the case where a second source was placed at $x = W$.